



Dissolved organic carbon-mediated controls dominate soil carbon mineralization in response to freeze-thaw cycles

Jixin Yan^{1,2}, Jinyang Zheng^{1,2,3}, Shuai Zhang^{1,2}, Mingming Wang^{1,2}, Ting Sun^{1,2}, Jiajun Mao^{1,2}, Zhongkui Luo^{1,2,*}

5 ¹State Key Laboratory of Soil Pollution Control and Safety, College of Environmental and Resource Sciences, Zhejiang University, Hangzhou 310058, China

²Key Laboratory of Environment Remediation and Ecological Health of Ministry of Education, Zhejiang University, Hangzhou 310058, China

³Current address: Department of Ecology, Evolution, and Organismal Biology, Iowa State University, Ames, IA, USA

10 *Correspondence to:* Zhongkui Luo (luozk@zju.edu.cn)

Abstract. Soil freeze-thaw cycles (FTCs) exert substantial effects on the mineralization of soil organic carbon (SOC), particularly in high-altitude and -latitude cold regions. Ongoing climate change is altering FTC frequency and duration, yet the responses of SOC mineralization to such changes remain poorly understood, limiting our ability to predict carbon cycle-climate feedbacks. Here, we incubated soils from two depths across three sites to quantify how FTC regimes regulate SOC mineralization and explore underlying controls. Across all treatments, we observed a pronounced thaw-induced pulse of CO₂ release, but more frequent freeze-thaw cycles led to more cumulative CO₂ release, given the same length of cumulative thaw days. Across treatments, mineralization was most strongly correlated with DOC and hydrolytic/oxidative enzyme activities, while being suppressed by mineralogical (free and amorphous Fe/Al oxides) and physical (aggregate-protected carbon) constraints. Partial correlations and path analyses revealed that DOC was the single most consistent predictor of mineralization, retaining its influence even when enzymatic, substrate quality, or mineralogical variables were controlled. Subsoil SOC mineralization was additionally shaped by molecular carbon composition and mineral protection. These findings reveal a vertical shift from DOC-mediated substrate accessibility to molecularly and physically constrained decomposition. Accounting for these depth-specific mechanisms will improve prediction of SOC-climate feedbacks under FTC shifts due to climate change.

1 Introduction

25 Soil freeze-thaw cycles (FTCs) are critical drivers of biogeochemical processes in seasonally and perennially frozen ecosystems, particularly across high-altitude and -latitude regions (Koven et al., 2020; Schuur et al., 2015). In the Northern Hemisphere, over 55% of the land area is subjected to seasonal FTCs (Lyon et al., 2022; Obu et al., 2019; Xiang et al., 2023). These cycles, caused by oscillations of soil temperature around 0 °C, induce periodic freezing and thawing, which in turn alters soil structure, nutrient mobility, microbial activity, and substrate accessibility. As such, FTCs exert strong control over the rate 30 and pathways of soil organic carbon (SOC) mineralization, with implications for both regional carbon budgets and global carbon-climate feedbacks (Tian et al., 2015). Climate change is rapidly modifying FTC regimes-altering their frequency,



intensity, and duration—due to accelerated warming in cold regions (Sorensen et al., 2018; Zhu et al., 2019). For example, warmer winters and reduced snow cover increase the likelihood of frequent FTCs even in formerly stable permafrost zones, potentially enhancing microbial decomposition and CO₂ emissions from SOC (Yang et al., 2024). Understanding how shifts 35 in FTC characteristics influence SOC mineralization is essential for improving projections of soil carbon turnover under future climate conditions.

Freeze-thaw cycles can alter SOC mineralization through a suite of tightly coupled biophysical processes. Physically, freezing leads to the formation of ice crystals that disrupt soil aggregates, increasing the exposure of formerly protected organic matter when thawing (Gao et al., 2015; Vaz et al., 1992). Thawing mobilizes soluble organic compounds and nutrients, 40 temporarily increasing the availability of substrates for microbial respiration. Biologically, repeated FTC events can cause microbial cell lysis during freeze events, releasing intracellular carbon and nutrients that fuel post-thaw microbial activity (Song et al., 2017). Extracellular enzyme profiles would be particularly important as they play a central role in catalysing carbon substrates, especially, complex organic polymers, and are sensitivity to FTCs (Feng et al., 2007). Although short-term freezing may have limited negative effects on microbial activity and community composition, and microbes can recovery 45 rapidly, long-term freezing may induce microbial dormancy or even death, inactivate extracellular enzymes, and/or shift microbial community composition, thereby altering microbial substrate strategies such as carbon use efficiency (Foster et al., 2016; Lí et al., 2024; Miura et al., 2019). To explicitly quantify SOC dynamics as impacted by FTCs, overall, it is important to elucidate the biophysical effects of FTCs on SOC mineralization which usually varies with soil physicochemical conditions (Kim et al., 2023; Liu et al., 2022; Song et al., 2017).

50 Despite increasing recognition of the importance of FTCs (Meisner et al., 2021; Sullivan et al., 2012), several critical knowledge gaps remain. Most existing studies have examined FTC effects in laboratory controlled conditions using simplified freeze-thaw treatments often with fixed durations, limited cycles, and surface soils without capturing the full spectrum of FTC conditions experienced in natural settings (Campbell et al., 2014). The duration of freezing and thawing within each cycle may strongly influence microbial responses, substrate availability, and the balance between cell damage and recovery, yet remains 55 poorly characterized. Furthermore, subsoil layers, which store the majority of SOC (Jobbág and Jackson, 2000; Li et al., 2020) and may experience distinct thermal and hydrological dynamics, are rarely included in FTC studies. Lastly, ecosystem-specific differences in soil texture, organic matter quality, and microbial communities could lead to divergent FTC responses, but comparative assessments across ecosystems are limited. These gaps hinder the ability of Earth system models to capture FTC-driven carbon dynamics with sufficient mechanistic details.

60 In this study, we conducted a laboratory incubation experiment to investigate how SOC mineralization responds to altered FTC patterns across soils from multiple ecosystems and depths. Specifically, we tested four FTC regimes that varied in the



duration of freeze and thaw phases in each cycle. This design allowed us to isolate the effects of FTC duration on microbial activity and SOC decomposition while accounting for spatial heterogeneity in soil properties. By quantifying SOC mineralization rates, cumulative CO₂ emissions, microbial enzyme activity, microbial carbon use efficiency (CUE), labile 65 carbon pools (e.g., dissolved organic carbon), and a series of other soil physicochemical properties, the objectives were to (1) determine how changes in freeze and thaw duration affect SOC mineralization; (2) identify controls over the response of SOC mineralization to FTC; and (3) evaluate whether these responses and controls differ across soil depths. By integrating measurements across physical, chemical, and biological domains, this study aims to advance mechanistic understanding of how evolving FTC patterns reshape soil carbon cycling and to improve model representation of carbon-climate feedbacks in 70 FTC-affected regions.

2 Materials and Methods

2.1 Study sites and soil sampling

Soil samples were collected from three sites along an elevational gradient (2400 m, 3400 m, and 4600 m) in southeastern Tibet, 75 China (29°16'–30°3'N, 94°44'–96°56'E). The mean annual temperature (MAT) at the three sites was 11.1, 3.4 and –1.3 °C, respectively, and the mean annual precipitation (MAP) was 844, 985 and 1057 mm, respectively. These sites differ in freeze-thaw regimes in terms of duration, intensity, and frequency, allowing assessment of the generality of freeze-thaw effects across contrasting baseline conditions. Detailed information on vegetation type and soil properties of the three sites is shown in Table S1.

In July 2023, at each elevation, three replicated plots (10 × 10 m), spaced ~100 m apart, were selected for soil sampling. 80 Within each plot, five points were randomly selected, and soil cores were extracted using a soil corer (3.7 cm diameter). Soil samples at two depth intervals (0–10 cm and 70–80 cm) were collected. The five samples from the same depth interval were thoroughly mixed to form a composite sample. The three composite samples from the three plots were treated as three replicates for each site (n = 3). All samples were put into an airtight bag and stored in a container with ice, and transferred to laboratory. In the laboratory, composite samples were divided into two portions: (1) fresh samples, which were stored at 4 °C for 85 incubation experiments and microbial properties; and (2) air-dried samples, which were air-dried at room temperature, and then sieved through a 2 mm mesh to remove gravel and roots for the analysis of soil organic carbon and other soil physicochemical (Table S2).



2.2 Measurements of soil organic carbon and physicochemical properties

A set of soil physicochemical properties, including soil organic carbon (SOC) with its chemical structure, total nitrogen (TN), 90 soil pH, soil texture, gravimetric water content, concentrations of iron and aluminum oxides and among others, were measured using air-dried samples. Specifically, soil water content was determined by oven-drying fresh subsamples at 105 °C to constant weight. SOC and TN were measured using an elemental analyzer (Vario EL Cube, Elementar, Germany) after removing 95 carbonates using dilute HCl. Soil pH was measured in a 1:2.5 (w:v) soil-water suspension using a pH electrode (Mettler Toledo, Switzerland). For soil texture, carbonates and organic matter were first removed using dilute HCl and H₂O₂, respectively, and then the dispersed samples were analyzed with a laser diffraction particle size analyzer (LS-CWM, OMEC, China) to determine 100 sand, silt and clay content. Free oxides (i.e., Fef, Alf) and amorphous oxides (Fea, Ala) of Fe and Al were extracted using dithionite–citrate–bicarbonate (DCB) and ammonium oxalate solutions, respectively, and their concentrations were measured by inductively coupled plasma optical emission spectrometry (ICP-OES; Optima 2000, PerkinElmer, USA). DCB and ammonium oxalate extractions followed by ICP-OES were used to measure Fef and Alf. Particulate organic carbon (POC) and 105 mineral-associated organic carbon (MAOC) were determined following the method of Six et al. (1998). Briefly, soil was dispersed with sodium hexametaphosphate and passed through a 0.053 mm sieve. Materials retained on the sieve was analyzed as POC, while the filtrate was used to quantify MAOC.

The chemical structure of SOC was analyzed using solid-state ¹³C cross-polarization magic-angle spinning nuclear 105 magnetic resonance (¹³C CPMAS NMR; Bruker Avance 300, Germany), following the procedure of Schmidt et al. (1997) and Mathers et al. (2002). Samples were first treated with 10% HF to remove paramagnetic materials, rinsed thoroughly, and sieved to <0.15 mm. NMR chemical shift regions were assigned as follows: 0-45 ppm (alkyl C), 45-110 ppm (O-alkyl C), 110-160 110 ppm (aromatic C), and 160-220 ppm (carboxyl C). The aromatic region was further divided into aryl C (110-145 ppm) and phenolic C (145-160 ppm). Ratios of alkyl C/O-alkyl C and hydrophobic C (alkyl + aromatic) to hydrophilic C (O-alkyl + carboxyl) were further calculated to characterize SOC quality (Mathers et al., 2007; Spaccini et al., 2002).

110 2.3 Incubation experiments and mineralization measurements

A 48-day laboratory incubation experiment was conducted to investigate the effect of freeze-thaw regimes on SOC mineralization by controlling the duration of freeze and thaw periods (Fig. S1): (1) LFLT – long freeze, long thaw: 12 days freeze followed by 12 days thaw (2 cycles in 48 days); (2) LFST – long freeze, short thaw: 12 days freeze followed by 4 days thaw (3 cycles); (3) SFLT – short freeze, long thaw: 4 days freeze followed by 12 days thaw (3 cycles); (4) SFST – short freeze, 115 short thaw: 4 days freeze followed by 4 days thaw (6 cycles).



For the incubation, 20 g of fresh soil was placed into 150 mL polyethylene jars (total = 72; four freeze-thaw regime treatments \times three sites \times two soil depths \times three replicates). All jars were pre-incubated at 10 °C for 10 days to stabilize microbial activity. Then, they were moved to incubator for incubation at –10 °C (freeze) and 10 °C (thaw) in sequence as the four freeze-thaw treatments described, with temperature fluctuations controlled within \pm 0.5 °C. Additionally, jars (500 ml, a 120 total of three soil sites \times two soil depths \times four freeze-thaw treatments = 24) with 300 g of fresh soil samples (wet weight) were incubated at the same freeze-thaw regimes for monitoring microbial properties, enzyme activities, and soil carbon properties at selected time points of soil mineralization measurements (section 2.4). For all jars, soil moisture was maintained at 60% of water-holding capacity by regularly weighing and, if required, adding distilled water. During the incubation, jars were sealed with gas-permeable but water-impermeable membranes to prevent anaerobic conditions and limit moisture loss.

125 Throughout the 48-day incubation period, SOC mineralization rate was measured during both the freeze and thaw phases at days 0.25 (i.e., 6 hours after the temperature treatment), 1, 2, 4, 7, and 12, when applicable. At each of the measurement time point, the 150 mL incubation jars were placed into an automatic soil respiration measurement system (PRI-8800, Pri-Eco, Beijing, China) (Liu et al., 2017; Nianpeng et al., 2013). Each measurement lasted 3 minutes at the current incubation temperature, and SOC mineralization rates were calculated as the slope of CO₂ concentration changes over time. These 130 measurements were linearly interpolated to estimate cumulative mineralization for the whole 48-day incubation, and for each phase (freeze and thaw).

2.4 Measurements of dissolved organic carbon and microbial properties

At time points aligned with SOC mineralization measurements, we quantified dissolved organic carbon (DOC), extracellular enzyme activities, microbial biomass carbon (MBC), and carbon use efficiency (CUE). For DOC and enzyme activities, soils 135 were sampled on days 1, 2, 4, 7 (in long phase only), and 12 (in long phase only). MBC and CUE were measured only on day 1 of each thaw period. For the LFLT and SFLT regimes, measurements of DOC, MBC, CUE, and enzyme activities were terminated after the first freeze–thaw cycle, whereas for the LFST and SFST regimes they were terminated after the third freeze-thaw cycle.

To quantify DOC, 1 g of fresh soil was extracted with 0.1 M K₂SO₄ at a soil-to-solution ratio of 1:10 (w/v). The extract 140 was filtered through a 0.45 µm membrane, and DOC concentration was measured using a total organic carbon analyzer (Multi N/C 3100, Analytik Jena, Germany). MBC was determined by the chloroform fumigation–extraction method (Vance et al., 1987). Briefly, 5 g of fresh soil was fumigated with ethanol-free chloroform for 24 h, while a parallel 5 g subsample remained unfumigated. Both samples were extracted with 20 ml of 0.5 M K₂SO₄ shaken for 30 minutes, and filtered through 0.45 µm



membranes. MBC was calculated as the difference in extractable organic carbon between the fumigated and unfumigated
145 samples, using a correction factor of 0.45 to account for incomplete biomass recovery.

CUE was determined using the ^{18}O -H₂O labelling method (Schwartz, 2007; Spohn et al., 2016). One gram of soil was split into two 0.5 g subsamples, each placed in a 2 ml screw-cap vial. One vial received 60 μl of ^{18}O -labeled water (20 atom% ^{18}O), and the control received the same volume of unlabeled water. After vertexing and centrifugation, samples were incubated at 10 °C for 24 h in sealed 50 ml jars. CO₂ concentrations were measured before and after incubation to assess microbial
150 respiration. Following incubation, soils were flash-frozen in liquid nitrogen and stored at -80 °C for DNA extraction. DNA was extracted using the MP Soil DNA Kit (FastDNATM Spin Kit for Soil, MP Biomedicals, Germany), with extended centrifugation to increase yield (Spohn et al., 2016). DNA was quantified using a NanoDrop spectrophotometer, dried in silver capsules at 60 °C for 48 h, and analyzed for ^{18}O enrichment by Isotope Ratio Mass Spectrometry (TC/EA-IRMS, Delta V Advantage, Thermo Fisher, Germany). CUE was calculated based on ^{18}O incorporation into microbial DNA relative to
155 cumulative CO₂ production.

Activities of four extracellular enzymes were measured to assess microbial function: two oxidative enzymes, including polyphenol oxidase (PPO) and peroxidase (POD), and two hydrolytic enzymes, including β -1,4-glucosidase (BG) and cellobiohydrolase (CBH). Enzyme activities were quantified using commercial ELISA kits (KeXing, Shanghai, China), following the manufacturer's protocol (Engvall and Perlmann, 1971; Uotila et al., 1981). For each assay, 1 g of fresh soil was
160 mixed thoroughly with 9 mL phosphate-buffered saline (PBS, pH 7.2-7.4). The suspension was centrifuged at 2-8 °C for ~20 min at 2000-3000 rpm, and the supernatant was collected. For the plate setup, 50 μL of standard solution were added to standard wells; sample wells received 40 μL of sample diluent plus 10 μL of soil supernatant; blank wells received no reagents. Plates were sealed and incubated at 37 °C for 30 mins. A 30 \times concentrated wash buffer was diluted 1:30 with distilled water. After removing the seal, liquid was discarded and the plate tapped dry; wells were filled with wash buffer, soaked for 30 s,
165 and emptied. This washing cycle was repeated five times. Then 50 μL of HRP-conjugated detection reagent were added, followed by the same incubation and washing steps. Subsequently, 50 μL of chromogenic substrate A were added to each well, followed by 50 μL of substrate B; plates were gently mixed and developed at 37 °C in the dark for 10 mins. Finally, 50 μL of stop solution were added, and absorbance was read at 450 nm using a microplate reader (BioTek Cytation 5, USA). Enzyme activity values were calculated from the standard calibration curve.

170 2.5 Statistical analyses

To evaluate how freeze-thaw treatments, soil origin, soil depth, measurement time, and freeze-thaw cycle number influenced SOC mineralization rates, we first performed a multivariate ANOVA, followed by Tukey's HSD tests for post-hoc



175 comparisons. Cumulative mineralization over the entire 48-day incubation, as well as cumulative mineralization during thaw and freeze phases, was compared among the four freeze-thaw treatments and between soil depths. Prior to all parametric analyses, data normality was assessed using Shapiro-Wilk tests and homogeneity of variance using Bartlett's tests; logarithmic transformation was applied when assumptions were not met.

180 To identify key covariates underlying mineralization responses, we focused initially on data from day 1 of the thaw period, the only time point at which MBC and CUE were measured. We used two-way ANOVA to characterize the effects of freeze-thaw treatment and soil depth on soil physicochemical and microbial variables, followed by Tukey's HSD for multiple comparisons. Within-treatment depth differences and within-depth treatment differences were summarized using significance groupings based on LSD tests with Bonferroni correction. We then fitted simple linear regressions of SOC mineralization rate (Rs) against each measured soil property and conducted univariate partial correlation analyses in which each variable was controlled in turn. These partial correlations quantify the unique association between Rs and a given predictor after removing variance attributable to another predictor, thereby revealing potential dependency relationships among covariates.

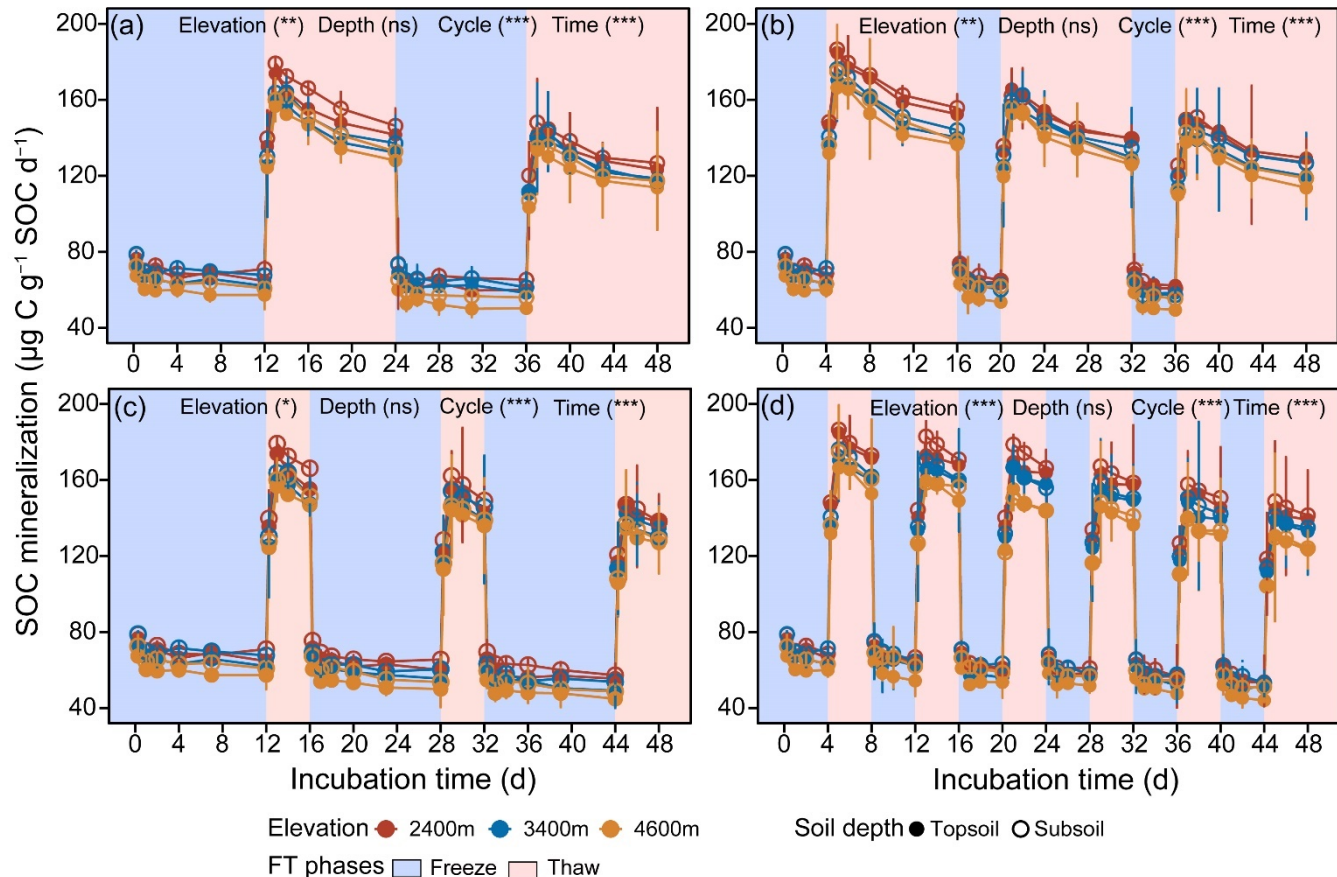
185 Variables most strongly associated with Rs on day 1 were then incorporated into linear mixed-effects models to test whether the relationships between Rs and selected predictors varied across freeze-thaw treatments or soil depths. In these models, freeze-thaw treatment and soil depth were treated as random intercepts. To examine whether the patterns observed on day 1 generalize across the thaw period, these mixed-effects analyses were repeated for additional time points where covariate data were available.

190 To disentangle the direct and indirect effects of freeze-thaw regimes on SOC mineralization, we applied partial least squares path modeling (PLS-PM) using all observations collected during thaw phases, with Rs as the response variable. Prior to model construction, we screened predictors using variance inflation factors (VIFs) and sequentially removed non-focal variables with $VIF > 10$ to reduce multicollinearity (Dormann et al., 2013). The categorical treatment factor (four freeze-thaw regimes) was retained by expanding it into dummy variables, which served as reflective indicators of a latent "Treatment" 195 construct, enabling the PLS-PM framework to represent treatment differences as a single exogenous driver (Hair et al., 2017). The final PLS-PM structure included six latent variables (Table S2). Separate models were fitted for topsoil and subsoil. Significance of structural path coefficients was evaluated using non-parametric bootstrap resampling (95% bootstrap confidence intervals). All variables were standardized prior to analysis. PLS-PM was conducted using the plspm package in R, and all statistical analyses were completed in R version 4.0.3 (<http://cran.r-project.org/>).



200 **3 Results**

3.1 The effects on mineralization rates

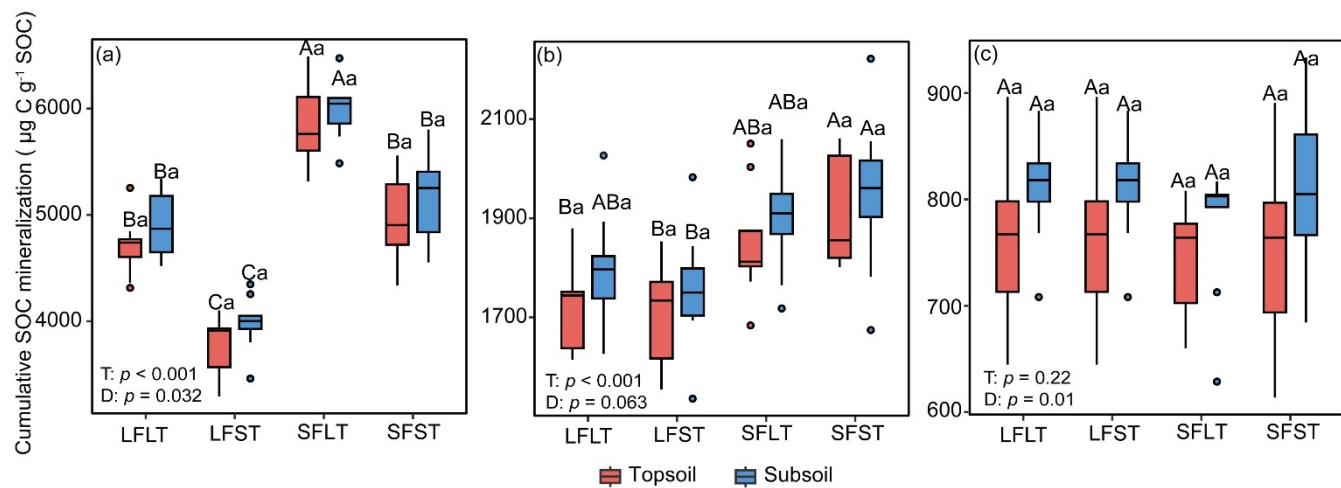


205 **Figure 1: Soil organic carbon (SOC) mineralization rate during freeze-thaw cycle incubation.** Soil was incubated for 48 days under two temperature conditions: -10°C (Freeze) and 10°C (Thaw). Four distinct freeze-thaw cycle patterns were designed to address knowledge gaps in previous studies, based on two cycle durations: 12-day (long) and 4-day (short). Panels a-d show the temporal dynamics of SOC mineralization under the four freeze-thaw regimes: (a) long freeze-long thaw (LFLT), (b) short freeze-long thaw (SFLT), (c) long freeze-short thaw (LFST), and (d) short freeze-short thaw (SFST). The blue and red background areas denote freezing (-10°C) and thawing (10°C) phases, respectively. Data points represent treatment means $\pm 1 \text{ SE}$ ($n = 3$). Significance tests compare elevations, soil depths, cycle number, and incubation time during thaw periods (*, $p < 0.05$; **, $p < 0.01$; ***, $p < 0.001$).

210 Carbon mineralization exhibited pronounced phase-dependent dynamics across all freeze-thaw regimes, soil depths, and sites (Fig. 1). During each thaw phase, SOC mineralization increased sharply, reaching its peak within one-occasionally two-days before declining. Peak thaw-phase mineralization ranged from 177.2 to $221.7 \mu\text{g C g}^{-1} \text{SOC d}^{-1}$ across treatments and soil origins. In contrast, mineralization during freezing remained comparatively low and stable (11.1 – $98.5 \mu\text{g C g}^{-1} \text{SOC d}^{-1}$), representing only 17.1–42.5% of thaw-phase peak rates.



215 Across successive freeze-thaw cycles, mineralization during both thaw and freeze phases declined in magnitude while
 maintaining their characteristic temporal patterns (Fig. 1). The magnitude of decline did not differ significantly between topsoil
 and subsoil ($p > 0.05$). For instance, under the LFLT treatment, cumulative mineralization in the second cycle was $13.7 \pm 2.8\%$
 (mean \pm SE) lower than in the first cycle. Comparable reductions were observed under LFST ($6.7 \pm 2.2\%$) and SFLT ($8.1 \pm$
 220 2.3%). The greatest attenuation occurred under SFST, where cumulative mineralization in the final cycle declined by $20.3 \pm$
 2.0% relative to the initial cycle.



225 **Figure 2: Cumulative soil organic carbon (SOC) mineralization under different freeze-thaw regimes and soil depths.** (a) Cumulative
 SOC mineralization over the full 48-day freeze-thaw incubation. (b) SOC mineralization over the same 12 cumulative thaw days. (c)
 SOC mineralization over the same 12 cumulative freeze days. Bars represent cumulative SOC mineralization for topsoil (0-10 cm)
 and subsoil (70-80 cm) under each freeze-thaw treatment. Error bars indicate ± 1 SE ($n = 18$). Uppercase letters denote significant
 differences among treatments within a given depth (Tukey's HSD), and lowercase letters indicate significant differences between
 depths within a given treatment.

Over the full 48-day incubation, cumulative mineralization differed markedly among freeze-thaw regimes. The SFST treatment produced the highest cumulative losses, followed by SFLT, LFLT, and LFST (Fig. 2a). This ordering closely 230 reflected the total number of thaw days associated with each treatment (36, 24, 24, and 12 days, respectively). In line with this pattern, cumulative mineralization during the freeze phase did not differ among treatments when compared over the same 12 cumulative freeze days ($p = 0.22$; 767.5 - 851.7 $\mu\text{g C g}^{-1}$ SOC; Fig. 2c). In contrast, substantial differences emerged during the thaw phase: cumulative mineralization over 12 cumulative thaw days was significantly higher under the SFST and SFLT treatments than under LFLT and LFST ($p < 0.001$; Fig. 2b). Across all freeze-thaw regimes, cumulative mineralization during 235 both freeze and thaw phases did not differ significantly between topsoil and subsoil (Fig. 2).

3.2 The effects on DOC, microbial properties and enzyme activities

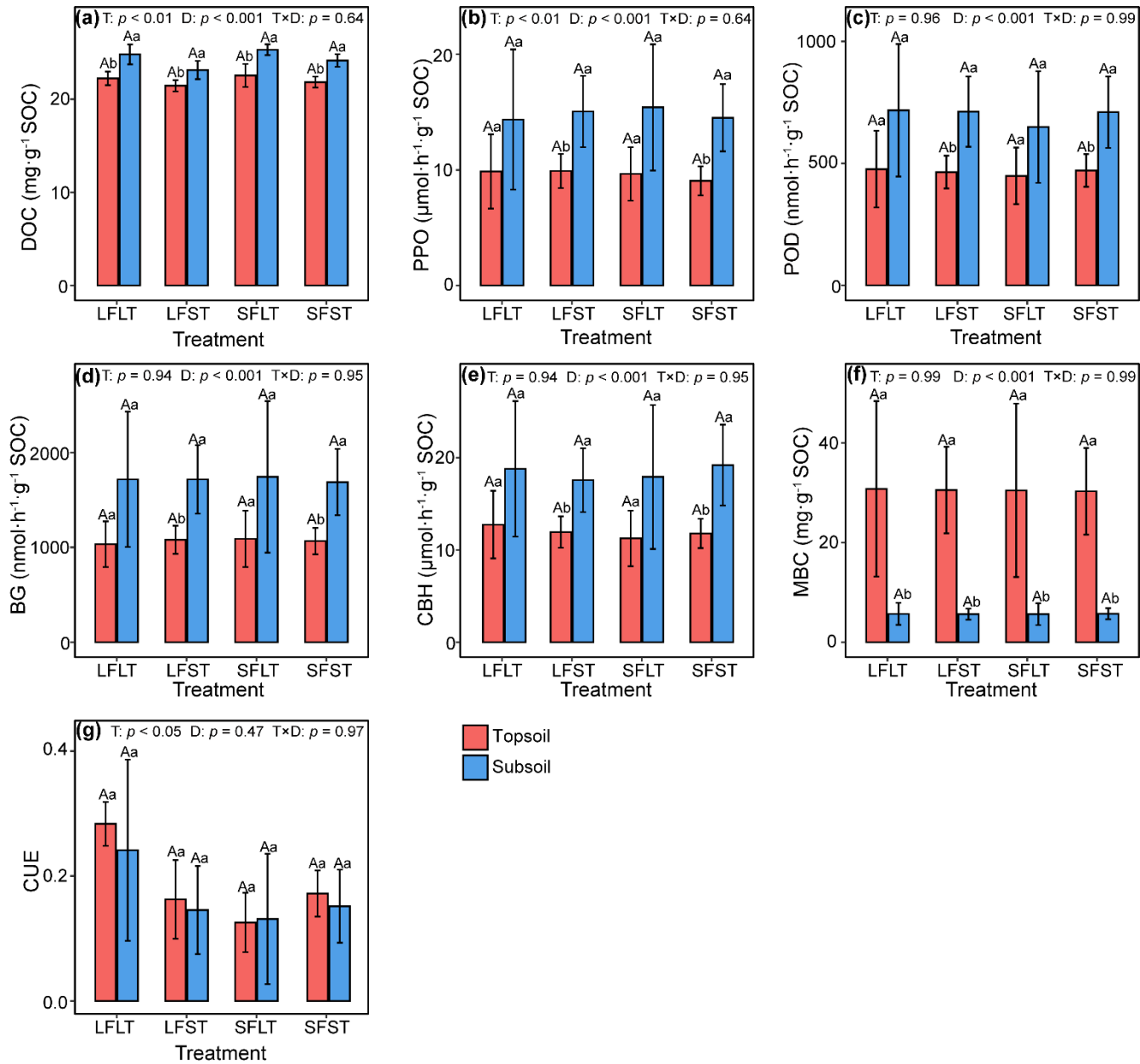


Figure 3: Effects of freeze-thaw regimes on dissolved organic, enzyme activities, and microbial properties across two soil depths. Panels (a-g) show dissolved organic carbon (DOC), polyphenol oxidase activity (PPO), peroxidase activity (POD), β -glucosidase activity (BG), cellobiohydrolase activity (CBH), microbial biomass carbon (MBC), and carbon use efficiency (CUE), respectively. Different uppercase letters indicate significant differences among treatments within the same soil depth, whereas different lowercase letters indicate significant differences between soil depths within the same treatment (Tukey's multiple comparison test).

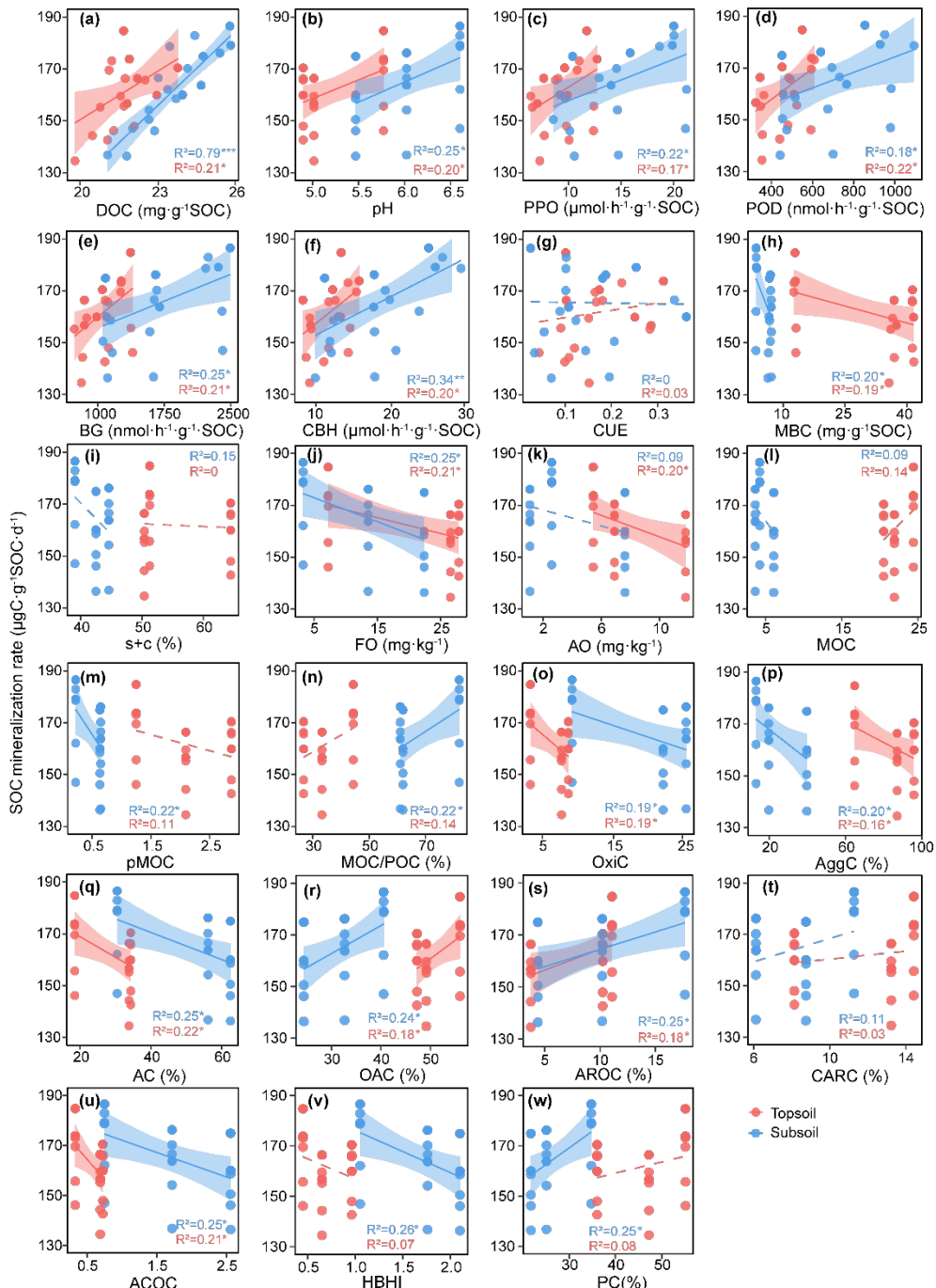


Figure 4: Relationships between soil properties and soil organic carbon (SOC) mineralization rate. Red and blue symbols represent the topsoil and subsoil, respectively. Solid lines indicate significant linear regressions, whereas dashed lines indicate non-significant relationships. R² shows the determination coefficient of the regression. Abbreviations of soil properties are defined in Table S2. Asterisks denote levels of statistical significance: *, $p < 0.05$; **, $p < 0.01$; ***, $p < 0.001$.

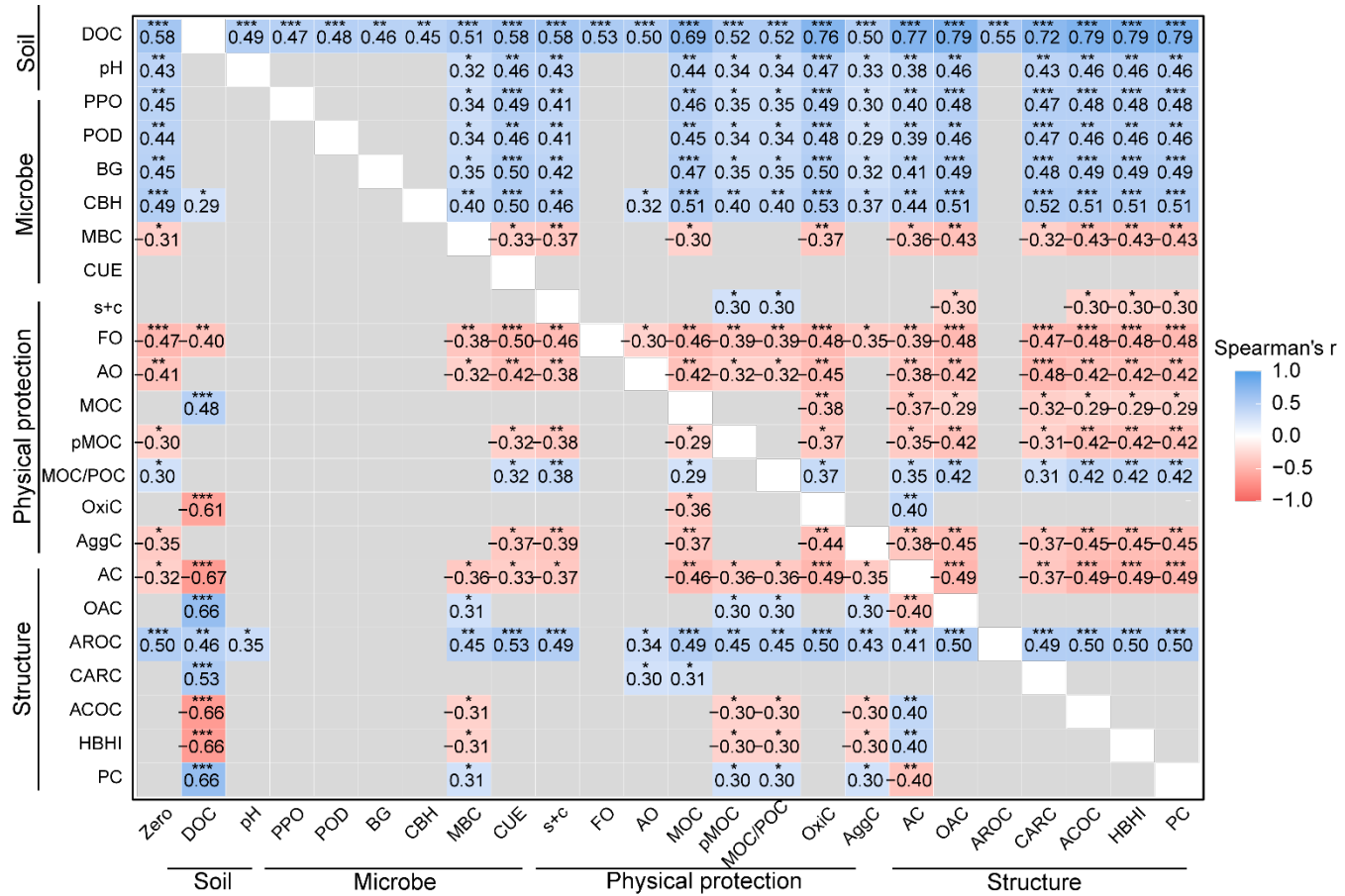


250 Freeze-thaw regimes exerted strong but variable effects on DOC and enzyme activities-two functional groups most directly linked to SOC mineralization. DOC showed a dynamic change over time, exhibiting pulsed patterns consistent with SOC mineralization rates (Fig. S3). On the first thawing day (Fig. 3; Fig. 4), DOC concentrations varied significantly among treatments, with the highest levels consistently observed under the high-frequency regime-SFLT. However, enzyme activities did not show significant differences across treatments in either the topsoil or subsoil. Hydrolytic enzymes (BG, CBH) and oxidative enzymes (PPO, POD) were not significantly elevated as DOC under high-frequency regimes. In contrast, enzyme activities under low-frequency regimes remained relatively low.

255 Microbial biomass carbon showed limited sensitivity to freeze-thaw treatments (Fig. 3; Fig. 4). Although some fluctuations occurred, treatment-level differences were small compared with those observed for DOC and enzymes, suggesting that freeze-thaw frequency influences microbial function and substrate supply more strongly than population size. Carbon use efficiency also remained stable across regimes, further indicating that the primary microbial responses to freeze-thaw cycling occurred through changes in substrate accessibility rather than shifts in microbial growth efficiency.



260 3.3 Predictors of mineralization rates



265 **Figure 5: Partial correlations (Spearman's r) of soil organic carbon (SOC) mineralization with soil physicochemical and biological properties. Correlation changes after controlling for each soil property is presented. Difference between zero-order and partial correlations indicates the level of dependency of the correlation between a given variable and the corresponding fluxes. The color and numbers indicate the strength and sign of the correlation. (No change in color between controlled variable and zero-order = no dependency; decrease/increase of color intensity = loss of/gain of correlation.) Statistical significance is indicated by asterisks (*, $p < 0.05$; **, $p < 0.01$; ***, $p < 0.001$). Abbreviations of the variables are explained in Table S2.**

270 After pooling the data from the first thawing day (on this day we have the most comprehensive measurements) across all freeze-thaw treatments, mineralization rates showed strong associations with indicators of substrate availability, molecular composition, and catalytic potential (Fig. 5). Positive correlations ($p < 0.05$) were observed with DOC (Spearman's $r = 0.58$), AROC ($r = 0.50$), and hydrolytic and oxidative enzymes including CBH ($r = 0.49$), BG ($r = 0.45$), PPO ($r = 0.45$), and POD ($r = 0.44$). Mineralization also increased modestly with soil pH ($r = 0.43$) and the MOC/POC ratio ($r = 0.30$, Fig. 5). In contrast, negative associations were detected with MBC ($r = -0.31$), free Fe/Al oxides ($r = -0.47$), amorphous oxides ($r = -0.41$), alkyl C ($r = -0.32$), and aggregate-protected carbon (AggC, $r = -0.35$), indicating stronger mineralogical and physical constraints where these fractions were more abundant.



Partial correlation analysis provided further insight into hierarchical relationships among DOC, enzymatic activity, and molecular structure (Fig. 5). After controlling for enzyme activities, all correlations except that with DOC became insignificant, suggesting that enzyme activity integrates information on microbial functioning and general substrate availability. In contrast, the correlation between mineralization and DOC remained significant regardless of which variables were controlled, 280 highlighting its distinct and dominant role as an immediately utilizable carbon pool. Controlling for DOC generated substantial shifts in associations with molecular C fractions. For instance, the negative correlation with alkyl C strengthened from $r = -0.32$ to -0.67 . Additional significant associations emerged with O-alkyl C ($r = 0.66$), carboxylic C ($r = 0.53$), the AC/OAC ratio ($r = -0.66$), the hydrophobic-hydrophilic ratio ($r = -0.66$), and polysaccharide C ($r = 0.66$), indicating that once DOC effects are accounted for, mineralization is strongly structured by the quality and functional-group distribution of remaining 285 SOC.

Separating the dataset by depth revealed striking vertical differentiation in the controls of SOC mineralization (Fig. S7). In both layers, DOC and enzyme activities remained significant zero-order predictors (Fig. S7), confirming their importance throughout the profile. However, the nature of secondary controls diverged with depth. Topsoil mineralization was primarily 290 associated with DOC and enzyme activity, whereas relationships with molecular C fractions were weak. By contrast, subsoil mineralization exhibited strong additional associations with C molecular composition (e.g., AC, OAC, ACOC, HBHI, PC), reflecting greater chemical and physical constraints on substrate decomposability at depth. Partial correlations reinforced this depth pattern. In the topsoil, controlling for DOC substantially altered relationships with multiple variables; the same effect appeared when controlling for soil texture (silt + clay). In the subsoil, however, controlling for pH, PPO, bulk density, CBH, free Fe/Al oxides, AggC, or molecular composition removed almost all remaining correlations, leaving DOC as the only 295 consistent predictor (Fig. S7). This pattern indicates a transition from a biologically dominated system in the topsoil to one where substrate chemistry and mineralogical protection exert stronger control in the subsoil.

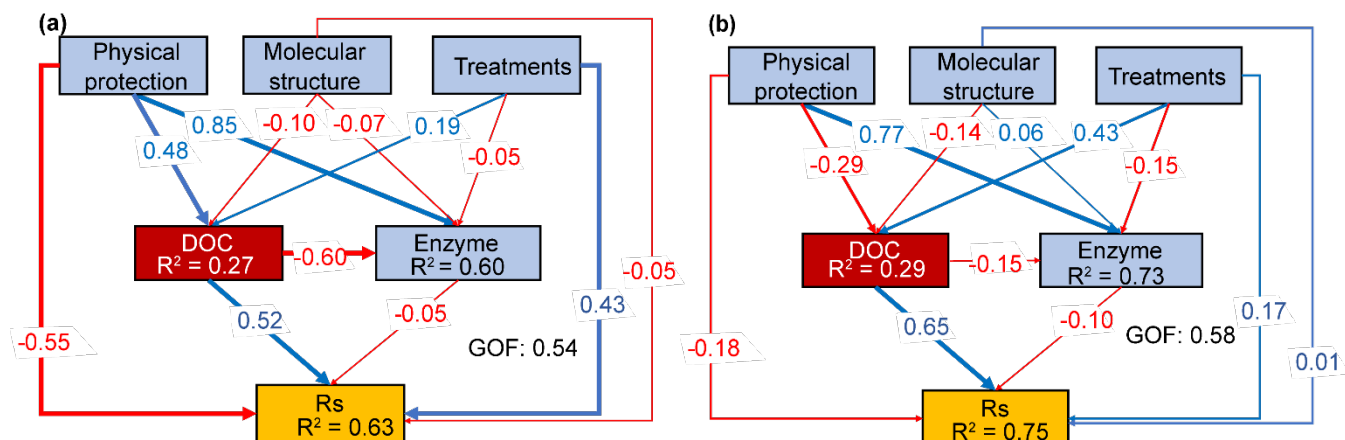


Figure 6: Path analysis results showing the direct and indirect controls of soil organic carbon (SOC) mineralization. Blue and red numbers indicate significant positive and negative relationships ($p < 0.05$). R^2 is the coefficient of determination, denoting the



300 **proportion of variance explained by the model. Panel (a) represents topsoil and panel (b) represents subsoil. Rs denotes the SOC
mineralization rate during the thawing phase of each freeze-thaw cycle. Indicators of the latent variables are listed in Table S2, and
their loadings are shown in Fig. S8.**

305 When expanding the analysis from the first thawing day to all thawing phases across freeze-thaw cycles, path analysis
further clarified these interacting controls (Fig. 6). DOC exerted strong direct effects on mineralization at both depths (path
coefficient $\rho = 0.52$ and 0.65 in the topsoil and subsoil, respectively). Physical protection had significant direct effects in both
310 layers but was much stronger in the topsoil. Freeze-thaw regimes influenced mineralization both directly and indirectly
through their effects on DOC and enzyme activities. Interestingly, the indirect pathways differed by depth: in the topsoil,
physical protection strongly increased DOC ($\rho = 0.48$) and enzyme activity ($\rho = 0.85$), whereas in the subsoil it primarily
enhanced enzyme activity ($\rho = 0.84$) while suppressing DOC, thereby affecting soil organic carbon mineralization. Moreover,
315 the relationship between DOC and enzyme activity showed the same direction but differed in strength across depths: in the
topsoil, they were strongly negatively correlated ($\rho = -0.60$), whereas in the subsoil the negative association was much weaker
($\rho = -0.15$), further revealing depth-dependent differences in microbial strategies and substrate limitation.

4 Discussion

4.1 The importance of FTC frequency

315 Our results show that SOC mineralization exhibits a sharp and immediate pulse upon thawing (Fig. 1), analogous to the Birch
effect observed when dry soils are rewetted (Canarini et al., 2020; Singh et al., 2023). This pulse may represent a rapid
reactivation of microbial metabolism and enzyme activity following the release of osmotic and physical constraints during
freezing (Chen et al., 2024; Köster et al., 2018; Wang et al., 2010). However, the magnitude of these thaw-induced pulses
320 declined across successive cycles, resulting in progressively lower cumulative mineralization during later thaw phases (Fig.
1). This attenuation likely reflects substrate depletion-given the absence of new carbon inputs in our experimental design –
and/or microbial acclimation to repeated stress of freeze (Deng et al., 2024; Li et al., 2024; Li et al., 2023).

325 A key finding is that FTC frequency strongly regulates cumulative SOC mineralization (Fig. 2). Soils subjected to many
short freeze-thaw oscillations (e.g., the SFLT regime) released substantially more CO₂ than those experiencing fewer, longer
cycles (e.g., LFLT), even when the cumulative number of thaw days was identical. Two complementary mechanisms likely
explain this pattern. First, each freeze event physically perturbs the soil matrix, disrupting aggregates, weakening organo-
mineral associations, and mobilizing DOC and fine particulate material that were previously protected. Multiple short cycles
may generate repeated substrate-release events, exposing new pools of labile and intermediate carbon that a single long thaw
is less effective at liberating (Liu et al., 2022; Patel et al., 2021). A long thaw may primarily exhaust the most accessible pools,



whereas repeated freeze-thaw transitions incrementally unlock additional protected fractions. Second, frequent but short thaws
330 may optimize microbial activation. If microbial reactivation time is short relative to thaw duration, each thaw enables a burst
of respiration before substantial resource depletion or physiological stress accumulates. In contrast, a single long thaw may
experience declining respiration over time due to substrate exhaustion, transient nutrient imbalances, or shifts in community
composition (Li et al., 2023; Lv et al., 2022; Rosinger et al., 2022). Moreover, repeated mild freeze-thaw events typically cause
335 less microbial mortality than a single prolonged or severe freeze, preserving an active decomposer community capable of
responding to successive pulses (Isobe et al., 2022; Liu et al., 2020; Pastore et al., 2023). Together, the results demonstrate
that FTC frequency is a key and independent driver of SOC turnover, rather than simply a function of thaw duration.

4.2 DOC as the primary and depth-invariant driver

A central finding of this study is that DOC emerged as the most consistent and powerful predictor of SOC mineralization
across all freeze-thaw regimes and environmental contexts represented by soil sampling sites and depths. DOC retained its
340 strong influence under every statistical evaluation (zero-order correlations, partial correlations, mixed-effects models, and path
analysis) while the effects of enzymatic, structural, and mineralogical variables often diminished or disappeared once DOC
was controlled. This convergence underscores the primacy of DOC as the proximal substrate controlling microbial respiration
during freeze-thaw transitions. This should be due to that DOC acts as a comprehensive indicator of substrate accessibility in
345 the context of FTCs, integrating contributions from physicochemical disturbance, microbial turnover, and extracellular
enzymatic depolymerization. First, freeze-thaw cycles directly modulate DOC availability by physically altering soil structure.
Freezing expands pore water and generates internal pressure that disrupts aggregates and weakens organo-mineral associations,
while thawing releases occluded carbon fractions into the dissolved phase (Kim et al., 2023; Wang et al., 2024). This physical
perturbation is complemented by biological processes: microbial cells ruptured by freezing liberate cytoplasmic solutes, amino
350 acids, and low-molecular-weight DOC, while membranes and necromass products provide additional labile substrates upon
thaw (Deng et al., 2024; Osei et al., 2024). Together, these processes create DOC pulses that microbes can rapidly metabolize,
explaining the immediate respiration spikes observed after thaw events (Fig. S3).

The depth-invariant importance of DOC is particularly notable given the stark contrasts in substrate quality, mineral
protection, and microbial biomass between topsoils and subsoils (Fig. 3, Fig. S4). Despite these differences, the slope of the
355 DOC-mineralization relationship remained statistically identical across depths. This suggests that once DOC becomes
available, microbial communities in depth layers exhibit comparable metabolic responsiveness, regardless of limitations
imposed by mineralogy or molecular composition. This finding has two major implications. First, microbial capacity to utilize
DOC is ubiquitous throughout the soil profile, even in deep horizons with lower biomass and reduced enzyme pools. Second,
depth-driven differences in respiration responses to FTCs arise primarily from factors that regulate DOC release, not from
differences in microbial utilization efficiency. In other words, depth determines how much DOC becomes available, but not



360 how effectively it is consumed once present. The partial correlation and path analyses strongly support this interpretation. When DOC was controlled, the explanatory power of enzyme activities, pH, mineral-associated carbon, aggregate protection, and molecular carbon fractions was substantially reduced, particularly in the topsoil. In the subsoil, controlling for DOC essentially eliminated all other predictors, leaving DOC as the only significant driver. This pattern indicates that other variables shape mineralization indirectly by influencing DOC production, stabilization, or mobilization rather than by directly
365 controlling metabolic turnover. Enzymes, for instance, become influential primarily by generating DOC from particulate or polymeric matter (Chen et al., 2025; Li et al., 2024). Mineral surfaces constrain mineralization chiefly by impeding DOC release, sorbing solutes, or shielding particulate C from depolymerization (Georgiou et al., 2022; Lavallee et al., 2020; Zhou et al., 2024). Even molecular composition mattered only when DOC availability was low, particularly in the DOC-limited
370 subsoil environment. These relationships collectively demonstrate that DOC sits at the nexus of microbial, chemical, and physical controls, functioning as the integrative control point of SOC mineralization under freeze-thaw conditions.

4.3 Depth-dependent regulation

While DOC emerged as the immediate and depth-invariant driver of SOC mineralization, our results reveal pronounced vertical differences in the secondary controls that regulate how FTCs shape substrate accessibility and microbial response. These depth-dependent constraints, spanning microbial functional capacity, mineral protection, and molecular structure, determine the
375 extent to which DOC can be mobilized, transformed, or retained during FTCs, and thus explain why topsoils and subsoils differ in their sensitivity to repeated freeze-thaw events. Subsoils showed strong coupling between DOC availability and enzyme activity, reflecting high microbial biomass, active extracellular enzyme pools, and abundant organic substrates (Chen et al., 2025; Deng et al., 2024). In this layer, hydrolytic and oxidative enzymes were significant correlates of mineralization, and partial correlations demonstrated that enzyme activity captured much of the variation attributable to substrate accessibility
380 and microbial functioning. This pattern indicates that subsoil microbes are well-positioned to rapidly depolymerize macromolecular organic matter and generate DOC during thawing events. Consequently, microbial catalytic capacity, rather than substrate chemistry or mineral protection, forms the dominant secondary constraint in subsoil horizons. FTCs therefore exert strong effects in subsoils by repeatedly triggering enzyme-mediated substrate release and rapid microbial activation.

In contrast, subsoils exhibited fundamentally different controls. Here, molecular carbon composition (e.g., alkyl C, O-
385 alkyl C, carboxylic C, polysaccharide C) and mineral protection (free and amorphous Fe/Al oxides, aggregate-protected C) were far more strongly associated with mineralization. Partial correlations revealed that controlling for mineralogical or structural properties eliminated nearly all remaining associations except DOC, indicating that physicochemical constraints dominate subsoil carbon dynamics. These constraints limit the release of DOC during FTCs by stabilizing organic matter on mineral surfaces and within aggregates, reducing both the quantity and quality of substrates accessible during thaw events
390 (Georgiou et al., 2022; Lavallee et al., 2020; Wang et al., 2024). Even though microbial utilization of DOC was efficient once



DOC was present, the primary bottleneck in subsoils was substrate liberation, not microbial metabolism. The depth-specific patterns uncovered in the path analysis further reinforce this distinction. In the topsoil, physical protection had a strong positive effect on DOC and a negative effect on enzyme activity, suggesting that localized protection can accumulate labile substrates while simultaneously suppressing enzymatic turnover. In subsoils, however, physical protection influenced mineralization 395 mostly through its positive effects on enzyme activity, with little effect on DOC. This implies that microbes in deeper horizons rely more heavily on persistent extracellular enzyme pools capable of mobilizing substrates slowly over time, and that FTC-induced structural disturbance is insufficient to overcome the dominant mineralogical constraints governing SOC availability.

4.4 Limitations and uncertainties

We highlight several limitations and uncertainties due to the laboratory incubation nature. First, the experimental design is still 400 relatively simple and cannot capture the complexity of FTC dynamics *in situ*. Particularly, the rate of temperature change in the incubator exceeds that of natural soil temperature changes in natural ambient climatic condition, which may lead to differences in the rate of ice crystal formation and aggregate disruption (Sahoo et al., 2025) and therefore altering substrate protection and accessibility. Second, the study did not assess the temporal dynamics of microbial community composition, albeit enzyme activities, CUE and microbial biomass carbon were monitored. The consequence of potential microbial 405 community changes would only manifest over long term (Feng et al., 2007; Ji et al., 2022). Recent studies have suggested that DOC released from freeze-induced cell lysis could preferentially stimulate the proliferation of r-strategist microbes, thereby shifting enzyme production patterns and substrate utilization preferences (Ernakovich et al., 2014; Yuan et al., 2022). In the absence of community composition data, we cannot determine whether the attenuation of CO₂ pulses observed in our experiment was driven by such community-level shifts. However, a plausible interpretation, consistent with earlier work, is 410 that repeated FTCs may gradually select for microbial taxa or physiological traits that are better adapted to recurring stress, thereby reducing the magnitude of respiration pulses over time. This potential mechanism requires direct microbial community profiling to be rigorously tested. For this reason, third, the 48-day incubation may be insufficient to extrapolate findings to directional FTC shifts in long-term. The response of stable SOC pools, such as mineral-associated organic carbon, typically requires months to years of microbial-mineral interactions (Haei et al., 2011; Turetsky et al., 2020). In addition, repeated FTCs 415 could induce functional adaptation or even evolutionary responses in microbial communities (e.g., upregulation of freeze-tolerance genes), which cannot be captured at the time scale of laboratory manipulation (Leyrer et al., 2024; Razavi et al., 2017)

5 Conclusions

Our results reveal that freeze-thaw cycles regulate SOC mineralization through a hierarchy of controls dominated by DOC 420 availability and modulated by depth-dependent microbial, chemical, and mineralogical constraints. Across all treatments and



soil layers, DOC emerged as the immediate and invariant driver of mineralization, acting as the proximal substrate pool that links physical disturbance, microbial activation, and enzymatic processing during thaw events. This central role of DOC explains the strong respiration pulses observed upon thawing and clarifies why FTC frequency, not simply the duration of thaw conditions, exerts such a pronounced influence on cumulative CO₂ release. Repeated freeze-thaw transitions mobilize
425 DOC through structural disruption and microbial turnover, while soils experiencing fewer, longer cycles lack these repeated substrate-release events. At the same time, the capacity of FTCs to generate DOC and sustain mineralization is shaped by vertical heterogeneity in soil properties. In topsoils, abundant microbial biomass and enzyme pools allow rapid conversion of particulate and polymeric organic matter into DOC (Gao et al., 2021; King et al., 2021; Li et al., 2024), amplifying the effects of frequent FTCs. In subsoils, by contrast, mineral protection and molecular composition constitute the dominant constraints,
430 limiting DOC release and reducing sensitivity to FTC frequency. This vertical transition from biologically mediated to chemically and physically constrained SOC turnover underscores the importance of depth-explicit perspectives when evaluating cold-season carbon dynamics.

The findings highlight the need for depth-explicit, mechanistic representations of FTCs in predicting their effects on soil carbon dynamics. First, FTCs should be treated as substrate-mobilizing events, not merely thermal perturbations. Second,
435 vertical heterogeneity across the soil profile must be properly captured: increasing FTC frequency is likely to accelerate topsoil carbon losses, while subsoils may remain buffered unless freeze penetration deepens with changing snow cover or warming-induced variability. Finally, in a climate where winter warming reduces freeze duration but increases freeze-thaw variability, greater FTC frequency may enhance cold-season carbon losses, with implications for high-latitude and mid-latitude carbon budgets.

440 **Data availability**

The data is available from the corresponding author upon reasonable request.

Author contributions

Z.L. conceived and designed the study; S.Z. conducted the field sampling; J.Y. and J.Z. were primarily responsible for the laboratory measurements and incubation experiments, with additional contributions from T.S. and J.M.; J.Y. assessed and
445 analyzed the data; Z.L. led the writing of the manuscript and interpretation of the results with contributions from J.Y.; M.W. and all authors contributed to discussions and manuscript revision.



Competing interests

The contact author has declared that none of the authors has any competing interests.

Acknowledgements

450 This research was financially supported by the National Natural Science Foundation of China (grant no. 32241036).

References

Campbell, J. L., Reinmann, A. B., and Templer, P. H.: Soil freezing effects on sources of nitrogen and carbon leached during snowmelt, *Soil Sci. Soc. Am. J.*, 78, 297–308, <https://doi.org/10.2136/sssaj2013.06.0218>, 2014.

Canarini, A., Wanek, W., Watzka, M., Sandén, T., Spiegel, H., Šantrůček, J., and Schnecker, J.: Quantifying microbial growth and carbon use efficiency in dry soil environments via¹⁸ O water vapor equilibration, *Glob. Change Biol.*, 26, 5333–5341, <https://doi.org/10.1111/gcb.15168>, 2020.

Chen, X., Cao, J., Sinsabaugh, R. L., Moorhead, D. L., Bardgett, R. D., Fanin, N., Nottingham, A. T., Zheng, X., and Chen, J.: Soil extracellular enzymes as drivers of soil carbon storage under nitrogen addition, *Biol. Rev.*, 100, 1716–1733, <https://doi.org/10.1111/brv.70021>, 2025.

460 Chen, Y., Han, M., Qin, W., Hou, Y., Zhang, Z., and Zhu, B.: Effects of whole-soil warming on CH₄ and N₂O fluxes in an alpine grassland, *Glob. Change Biol.*, 30, e17033, <https://doi.org/10.1111/gcb.17033>, 2024.

Deng, Y., Li, X., Shi, F., and Zhang, Y.: Divergent controlling factors of freeze–thaw-induced changes in dissolved organic carbon and microbial biomass carbon between topsoil and subsoil of cold alpine grasslands, *CATENA*, 241, 108063, <https://doi.org/10.1016/j.catena.2024.108063>, 2024.

465 Dormann, C. F., Elith, J., Bacher, S., Buchmann, C., Carl, G., Carré, G., Marquéz, J. R. G., Gruber, B., Lafourcade, B., Leitão, P. J., Münkemüller, T., McClean, C., Osborne, P. E., Reineking, B., Schröder, B., Skidmore, A. K., Zurell, D., and Lautenbach, S.: Collinearity: A review of methods to deal with it and a simulation study evaluating their performance, *Ecography*, 36, 27–46, <https://doi.org/10.1111/j.1600-0587.2012.07348.x>, 2013.

Engvall, E. and Perlmann, P.: Enzyme-linked immunosorbent assay (ELISA) quantitative assay of immunoglobulin G, *470 Immunochemistry*, 8, 871–874, [https://doi.org/10.1016/0019-2791\(71\)90454-X](https://doi.org/10.1016/0019-2791(71)90454-X), 1971.

Ernakovich, J. G., Hopping, K. A., and Berdanier, A. B.: Predicted responses of arctic and alpine ecosystems to altered seasonality under climate change, *Glob. Change Biol.*, 20, 3256–3269, 2014.

Feng, X., Nielsen, L. L., and Simpson, M. J.: Responses of soil organic matter and microorganisms to freeze–thaw cycles, *Soil Biol. Biochem.*, 39, 2027–2037, 2007.



475 Foster, A., Jones, D. L., Cooper, E. J., and Roberts, P.: Freeze–thaw cycles have minimal effect on the mineralisation of low molecular weight, dissolved organic carbon in arctic soils, *Polar Biol.*, 39, 2387–2401, <https://doi.org/10.1007/s00300-016-1914-1>, 2016.

Gao, D., Bai, E., Yang, Y., Zong, S., and Hagedorn, F.: A global meta-analysis on freeze-thaw effects on soil carbon and phosphorus cycling, *Soil Biol. Biochem.*, 159, 108283, <https://doi.org/10.1016/j.soilbio.2021.108283>, 2021.

480 Gao, Y., Zeng, X., Xie, Q., and Ma, X.: Release of carbon and nitrogen from alpine soils during thawing periods in the eastern Qinghai-Tibet Plateau, *Water. Air. Soil Pollut.*, 226, 1–9, 2015.

Georgiou, K., Jackson, R. B., Vindušková, O., Abramoff, R. Z., Ahlström, A., Feng, W., Harden, J. W., Pellegrini, A. F. A., Polley, H. W., Soong, J. L., Riley, W. J., and Torn, M. S.: Global stocks and capacity of mineral-associated soil organic carbon, *Nat. Commun.*, 13, 3797, <https://doi.org/10.1038/s41467-022-31540-9>, 2022.

485 Haei, M., Rousk, J., Ilstedt, U., Öquist, M., Bååth, E., and Laudon, H.: Effects of soil frost on growth, composition and respiration of the soil microbial decomposer community, *Soil Biol. Biochem.*, 43, 2069–2077, 2011.

Hair, J. F., Hult, G. T. M., Ringle, C. M., and Sarstedt, M.: A primer on partial least squares structural equation modeling (PLS-SEM), Second edition., SAGE, Los Angeles London New Delhi Singapore Washington DC Melbourne, 363 pp., 2017.

490 Isobe, K., Oka, H., Watanabe, T., Tateno, R., Senoo, K., and Shibata, H.: Soil microbial community response to winter climate change is phylogenetically conserved and highly resilient in a cool-temperate forest, *Soil Biol. Biochem.*, 165, 108499, <https://doi.org/10.1016/j.soilbio.2021.108499>, 2022.

Ji, X., Liu, M., Yang, J., and Feng, F.: Meta-analysis of the impact of freeze–thaw cycles on soil microbial diversity and C and N dynamics, *Soil Biol. Biochem.*, 168, 108608, <https://doi.org/10.1016/j.soilbio.2022.108608>, 2022.

Jobbágy, E. G. and Jackson, R. B.: The vertical distribution of soil organic carbon and its relation to climate and vegetation, *495 Ecol. Appl.*, 10, 423–436, [https://doi.org/10.1890/1051-0761\(2000\)010%255B0423:TVDOSO%255D2.0.CO;2](https://doi.org/10.1890/1051-0761(2000)010%255B0423:TVDOSO%255D2.0.CO;2), 2000.

Kim, Y. J., Kim, J., and Jung, J. Y.: Responses of dissolved organic carbon to freeze–thaw cycles associated with the changes in microbial activity and soil structure, *The Cryosphere*, 17, 3101–3114, <https://doi.org/10.5194/tc-17-3101-2023>, 2023.

King, A. E., Rezanezhad, F., and Wagner-Riddle, C.: Evidence for microbial rather than aggregate origin of substrates fueling freeze-thaw induced N2O emissions, *Soil Biol. Biochem.*, 160, 108352, <https://doi.org/10.1016/j.soilbio.2021.108352>, 2021.

500 Köster, E., Köster, K., Berninger, F., Prokushkin, A., Aaltonen, H., Zhou, X., and Pumpanen, J.: Changes in fluxes of carbon dioxide and methane caused by fire in siberian boreal forest with continuous permafrost, *J. Environ. Manage.*, 228, 405–415, <https://doi.org/10.1016/j.jenvman.2018.09.051>, 2018.

Koven, C. D., Knox, R. G., Fisher, R. A., Chambers, J. Q., Christoffersen, B. O., Davies, S. J., Dett, M., Dietze, M. C., Faybushenko, B., Holm, J., Huang, M., Kovenock, M., Kueppers, L. M., Lemieux, G., Massoud, E., McDowell, N. G., Muller-505 Landau, H. C., Needham, J. F., Norby, R. J., Powell, T., Rogers, A., Serbin, S. P., Shuman, J. K., Swann, A. L. S., Varadharajan, C., Walker, A. P., Wright, S. J., and Xu, C.: Benchmarking and parameter sensitivity of physiological and vegetation dynamics using the functionally assembled terrestrial ecosystem simulator (FATES) at barro colorado island, panama, *Biogeosciences*, 17, 3017–3044, <https://doi.org/10.5194/bg-17-3017-2020>, 2020.



510 Lavallee, J. M., Soong, J. L., and Cotrufo, M. F.: Conceptualizing soil organic matter into particulate and mineral-associated forms to address global change in the 21st century, *Glob. Change Biol.*, 26, 261–273, <https://doi.org/10.1111/gcb.14859>, 2020.

Leyrer, V., Poll, C., Wirsching, J., Kandeler, E., and Marhan, S.: Warming persistently stimulates respiration from an arable soil over a decade, regardless of reduced summer precipitation, *Soil Biol. Biochem.*, 194, 109439, <https://doi.org/10.1016/j.soilbio.2024.109439>, 2024.

515 Li, J., Wu, J., Yu, J., Wang, K., Li, J., Cui, Y., Shangguan, Z., and Deng, L.: Soil enzyme activity and stoichiometry in response to precipitation changes in terrestrial ecosystems, *Soil Biol. Biochem.*, 191, 109321, <https://doi.org/10.1016/j.soilbio.2024.109321>, 2024.

Lí, J., Hicks, L. C., Brangarí, A. C., Tájmel, D., Cruz-Paredes, C., and Rousk, J.: Subarctic winter warming promotes soil microbial resilience to freeze–thaw cycles and enhances the microbial carbon use efficiency, *Glob. Change Biol.*, 30, e17040, <https://doi.org/10.1111/gcb.17040>, 2024.

520 Li, J.-T., Xu, H., Hicks, L. C., Brangarí, A. C., and Rousk, J.: Comparing soil microbial responses to drying–rewetting and freezing–thawing events, *Soil Biol. Biochem.*, 178, 108966, <https://doi.org/10.1016/j.soilbio.2023.108966>, 2023.

Li, X., Xie, J., Zhang, Q., Lyu, M., Xiong, X., Liu, X., Lin, T., and Yang, Y.: Substrate availability and soil microbes drive temperature sensitivity of soil organic carbon mineralization to warming along an elevation gradient in subtropical Asia, *Geoderma*, 364, 114198, <https://doi.org/10.1016/j.geoderma.2020.114198>, 2020.

525 Liu, H., Rezanezhad, F., Zak, D., Li, X., and Lennartz, B.: Freeze–thaw cycles alter soil hydro–physical properties and dissolved organic carbon release from peat, *Front. Environ. Sci.*, 10, 930052, <https://doi.org/10.3389/fenvs.2022.930052>, 2022.

Liu, K., Xu, Y., Feng, W., Zhang, X., Yao, S., and Zhang, B.: Modeling the dynamics of protected and primed organic carbon in soil and aggregates under constant soil moisture following litter incorporation, *Soil Biol. Biochem.*, 151, 108039, <https://doi.org/10.1016/j.soilbio.2020.108039>, 2020.

530 Liu, Y., He, N., Zhu, J., Xu, L., Yu, G., Niu, S., Sun, X., and Wen, X.: Regional variation in the temperature sensitivity of soil organic matter decomposition in China’s forests and grasslands, *Glob. Change Biol.*, 23, 3393–3402, <https://doi.org/10.1111/gcb.13613>, 2017.

Lv, Z., Gu, Y., Chen, S., Chen, J., and Jia, Y.: Effects of autumn diurnal freeze–thaw cycles on soil bacteria and greenhouse gases in the permafrost regions, *Front. Microbiol.*, 13, 1056953, <https://doi.org/10.3389/fmich.2022.1056953>, 2022.

535 Lyon, C., Saupe, E. E., Smith, C. J., Hill, D. J., Beckerman, A. P., Stringer, L. C., Marchant, R., McKay, J., Burke, A., O’Higgins, P., Dunhill, A. M., Allen, B. J., Riel-Salvatore, J., and Aze, T.: Climate change research and action must look beyond 2100, *Glob. Change Biol.*, 28, 349–361, <https://doi.org/10.1111/gcb.15871>, 2022.

Mathers, N. J., Xu, Z., Berners-Price, S. J., Senake Perera, M. C., and Saffigna, P. G.: Hydrofluoric acid pre-treatment for improving ^{13}C CPMAS NMR spectral quality of forest soils in south-east queensland, australia, *Aust. J. Soil Res.*, 40, 665–540 674, <https://doi.org/10.1071/SR01073>, 2002.



Mathers, N. J., Jalota, R. K., Dalal, R. C., and Boyd, S. E.: ¹³C-NMR analysis of decomposing litter and fine roots in the semi-arid mulga lands of southern queensland, *Soil Biol. Biochem.*, 39, 993–1006, <https://doi.org/10.1016/j.soilbio.2006.11.009>, 2007.

Meisner, A., Snoek, B. L., Nesme, J., Dent, E., Jacquiod, S., Classen, A. T., and Priemé, A.: Soil microbial legacies differ 545 following drying–rewetting and freezing–thawing cycles, *ISME J.*, 15, 1207–1221, <https://doi.org/10.1038/s41396-020-00844-3>, 2021.

Miura, M., Jones, T. G., Hill, P. W., and Jones, D. L.: Freeze–thaw and dry–wet events reduce microbial extracellular enzyme activity, but not organic matter turnover in an agricultural grassland soil, *Appl. Soil Ecol.*, 144, 196–199, <https://doi.org/10.1016/j.apsoil.2019.08.002>, 2019.

550 Nianpeng, H., Ruomeng, W., Yang, G., Jingzhong, D., Xuefa, W., and Guirui, Y.: Changes in the temperature sensitivity of SOM decomposition with grassland succession: implications for soil C sequestration, *Ecol. Evol.*, 3, 5045–5054, <https://doi.org/10.1002/ece3.881>, 2013.

Obu, J., Westermann, S., Bartsch, A., Berdnikov, N., Christiansen, H. H., Dashtseren, A., Delaloye, R., Elberling, B., Etzelmüller, B., Kholodov, A., Khomutov, A., Kääb, A., Leibman, M. O., Lewkowicz, A. G., Panda, S. K., Romanovsky, V., 555 Way, R. G., Westergaard-Nielsen, A., Wu, T., Yamkhin, J., and Zou, D.: Northern hemisphere permafrost map based on TTOP modelling for 2000–2016 at 1 km² scale, *Earth-Sci. Rev.*, 193, 299–316, <https://doi.org/10.1016/j.earscirev.2019.04.023>, 2019. Osei, A. K., Rezanezhad, F., and Oelbermann, M.: Impact of freeze–thaw cycles on greenhouse gas emissions in marginally productive agricultural land under different perennial bioenergy crops, *J. Environ. Manage.*, 357, 120739, <https://doi.org/10.1016/j.jenvman.2024.120739>, 2024.

560 Pastore, M. A., Classen, A. T., English, M. E., Frey, S. D., Knorr, M. A., Rand, K., and Adair, E. C.: Soil microbial legacies influence freeze–thaw responses of soil, *Funct. Ecol.*, 37, 1055–1066, <https://doi.org/10.1111/1365-2435.14273>, 2023.

Patel, K. F., Tatariw, C., MacRae, J. D., Ohno, T., Nelson, S. J., and Fernandez, I. J.: Repeated freeze–thaw cycles increase extractable, but not total, carbon and nitrogen in a maine coniferous soil, *Geoderma*, 402, 115353, 2021.

Razavi, B. S., Liu, S., and Kuzyakov, Y.: Hot experience for cold-adapted microorganisms: Temperature sensitivity of soil 565 enzymes, *Soil Biol. Biochem.*, 105, 236–243, <https://doi.org/10.1016/j.soilbio.2016.11.026>, 2017.

Rosinger, C., Clayton, J., Baron, K., and Bonkowski, M.: Soil freezing–thawing induces immediate shifts in microbial and resource stoichiometry in luvisol soils along a postmining agricultural chronosequence in western germany, *Geoderma*, 408, 115596, 2022.

Sahoo, M., Bentley, P., Smith, A., Blackbourn, P., Howarth, K., Bau, D., and Thornton, S.: A laboratory-scale physical model 570 for freeze–thaw studies in soil columns under simulated climate change conditions, *Environ. Sci. Pollut. Res.*, 32, 5293–5301, <https://doi.org/10.1007/s11356-025-36053-8>, 2025.

Schmidt, M. W. I., Knicker, H., Hatcher, P. G., and Kogel-Knabner, I.: Improvement of ¹³ C and ¹⁵ N CPMAS NMR spectra of bulk soils, particle size fractions and organic material by treatment with 10% hydrofluoric acid, *Eur. J. Soil Sci.*, 48, 319–328, <https://doi.org/10.1111/j.1365-2389.1997.tb00552.x>, 1997.



575 Schuur, E. A., McGuire, A. D., Schädel, C., Grosse, G., Harden, J. W., Hayes, D. J., Hugelius, G., Koven, C. D., Kuhry, P., and Lawrence, D. M.: Climate change and the permafrost carbon feedback, *Nature*, 520, 171–179, 2015.

Schwartz, E.: Characterization of growing microorganisms in soil by stable isotope probing with H_2^{18}O , *Appl. Environ. Microbiol.*, 73, 2541–2546, <https://doi.org/10.1128/AEM.02021-06>, 2007.

Singh, S., Mayes, M. A., Kivlin, S. N., and Jagadamma, S.: How the birch effect differs in mechanisms and magnitudes due 580 to soil texture, *Soil Biol. Biochem.*, 179, 108973, <https://doi.org/10.1016/j.soilbio.2023.108973>, 2023.

Six, J., Elliott, E. T., Paustian, K., and Doran, J. W.: Aggregation and soil organic matter accumulation in cultivated and native grassland soils, *Soil Sci. Soc. Am. J.*, 62, 1367–1377, <https://doi.org/10.2136/sssaj1998.03615995006200050032x>, 1998.

Song, Y., Zou, Y., Wang, G., and Yu, X.: Altered soil carbon and nitrogen cycles due to the freeze-thaw effect: A meta-analysis, *Soil Biol. Biochem.*, 109, 35–49, <https://doi.org/10.1016/j.soilbio.2017.01.020>, 2017.

585 Sorensen, P. O., Finzi, A. C., Giasson, M.-A., Reinmann, A. B., Sanders-DeMott, R., and Templer, P. H.: Winter soil freeze-thaw cycles lead to reductions in soil microbial biomass and activity not compensated for by soil warming, *Soil Biol. Biochem.*, 116, 39–47, <https://doi.org/10.1016/j.soilbio.2017.09.026>, 2018.

Spaccini, R., Piccolo, A., Conte, P., Haberhauer, G., and Gerzabek, M. H.: Increased soil organic carbon sequestration through 590 hydrophobic protection by humic substances, *Soil Biol. Biochem.*, 34, 1839–1851, [https://doi.org/10.1016/S0038-0717\(02\)00197-9](https://doi.org/10.1016/S0038-0717(02)00197-9), 2002.

Spohn, M., Klaus, K., Wanek, W., and Richter, A.: Microbial carbon use efficiency and biomass turnover times depending on soil depth – implications for carbon cycling, *Soil Biol. Biochem.*, 96, 74–81, <https://doi.org/10.1016/j.soilbio.2016.01.016>, 2016.

Sullivan, B. W., Dore, S., Montes-Helu, M. C., Kolb, T. E., and Hart, S. C.: Pulse emissions of carbon dioxide during snowmelt 595 at a high-elevation site in Northern Arizona, USA, *Arct. Antarct. Alp. Res.*, 44, 247–254, 2012.

Tian, H., Lu, C., Yang, J., Banger, K., Huntzinger, D. N., Schwalm, C. R., Michalak, A. M., Cook, R., Ciais, P., Hayes, D., Huang, M., Ito, A., Jain, A. K., Lei, H., Mao, J., Pan, S., Post, W. M., Peng, S., Poulter, B., Ren, W., Ricciuto, D., Schaefer, K., Shi, X., Tao, B., Wang, W., Wei, Y., Yang, Q., Zhang, B., and Zeng, N.: Global patterns and controls of soil organic carbon dynamics as simulated by multiple terrestrial biosphere models: Current status and future directions, *Glob. Biogeochem. Cycles*, 29, 775–792, <https://doi.org/10.1002/2014GB005021>, 2015.

Turetsky, M. R., Abbott, B. W., Jones, M. C., Anthony, K. W., Olefeldt, D., Schuur, E. A. G., Grosse, G., Kuhry, P., Hugelius, G., Koven, C., Lawrence, D. M., Gibson, C., Sannel, A. B. K., and McGuire, A. D.: Carbon release through abrupt permafrost thaw, *Nat. Geosci.*, 13, 138–143, <https://doi.org/10.1038/s41561-019-0526-0>, 2020.

Uotila, M., Ruoslahti, E., and Engvall, E.: Two-site sandwich enzyme immunoassay with monoclonal antibodies to human 605 alpha-fetoprotein, *J. Immunol. Methods*, 42, 11–15, [https://doi.org/10.1016/0022-1759\(81\)90219-2](https://doi.org/10.1016/0022-1759(81)90219-2), 1981.

Vance, E. D., Brookes, P. C., and Jenkinson, D. S.: An extraction method for measuring soil microbial biomass C, *Soil Biol. Biochem.*, 19, 703–707, [https://doi.org/10.1016/0038-0717\(87\)90052-6](https://doi.org/10.1016/0038-0717(87)90052-6), 1987.



Vaz, M. D. R., Edwards, A. C., Shand, C. A., and Cresser, M.: Determination of dissolved organic phosphorus in soil solutions by an improved automated photo-oxidation procedure, *Talanta*, 39, 1479–1487, [https://doi.org/10.1016/0039-9140\(92\)80129-2](https://doi.org/10.1016/0039-9140(92)80129-2), 1992.

610 Wang, F., Gao, S., Zhang, K., Li, H., Bai, L., Huang, Z., and Mi, C.: Effects of nitrogen application on N₂O flux from fluvo-aquic soil subject to freezing-thawing process, *Agric. Sci. China*, 9, 577–582, [https://doi.org/10.1016/S1671-2927\(09\)60131-0](https://doi.org/10.1016/S1671-2927(09)60131-0), 2010.

Wang, G., Peng, Y., Chen, L., Abbott, B. W., Ciais, P., Kang, L., Liu, Y., Li, Q., Peñuelas, J., Qin, S., Smith, P., Song, Y.,
615 Strauss, J., Wang, J., Wei, B., Yu, J., Zhang, D., and Yang, Y.: Enhanced response of soil respiration to experimental warming upon thermokarst formation, *Nat. Geosci.*, <https://doi.org/10.1038/s41561-024-01440-2>, 2024.

Xiang, D., Wang, G., Tian, J., and Li, W.: Global patterns and edaphic-climatic controls of soil carbon decomposition kinetics predicted from incubation experiments, *Nat. Commun.*, 14, 2171, <https://doi.org/10.1038/s41467-023-37900-3>, 2023.

Yang, X., Chu, D., Hu, H., Deng, W., Chen, J., and Guo, S.: Effects of land-use type and salinity on soil carbon mineralization
620 in coastal areas of northern Jiangsu province, *Sustainability*, 16, 3285, <https://doi.org/10.3390/su16083285>, 2024.

Yuan, M., Na, M., Hicks, L. C., and Rousk, J.: Will a legacy of enhanced resource availability accelerate the soil microbial response to future climate change?, *Soil Biol. Biochem.*, 165, 108492, <https://doi.org/10.1016/j.soilbio.2021.108492>, 2022.

Zhou, Z., Ren, C., Wang, C., Delgado-Baquerizo, M., Luo, Y., Luo, Z., Du, Z., Zhu, B., Yang, Y., Jiao, S., Zhao, F., Cai, A.,
625 Yang, G., and Wei, G.: Global turnover of soil mineral-associated and particulate organic carbon, *Nat. Commun.*, 15, 5329, <https://doi.org/10.1038/s41467-024-49743-7>, 2024.

Zhu, L., Ives, A. R., Zhang, C., Guo, Y., and Radeloff, V. C.: Climate change causes functionally colder winters for snow cover-dependent organisms, *Nat. Clim. Change*, 9, 886–893, <https://doi.org/10.1038/s41558-019-0588-4>, 2019.